Hydrology and Earth System Sciences Discussions

Papers published in *Hydrology and Earth System Sciences Discussions* are under open-access review for the journal *Hydrology and Earth System Sciences*

A distributed continuous simulation model to identify critical source areas of phosphorus at the catchment scale: model description

B. K. Koo, S. M. Dunn, and R. C. Ferrier

The Macaulay Institute, Craigiebuckler, Aberdeen AB15 8QH, UK

Correspondence to: B. K. Koo (b.koo@macaulay.ac.uk)

Title Page

Abstract	Introduction
Conclusions	References
Tables	Figures

|◄ | ►|

◄ | ►

Back | Close

Full Screen / Esc

Print Version

Interactive Discussion

EGU

A distributed continuous simulation model

B. K. Koo et al.

Abstract

This paper presents CAMEL (Chemicals from Agricultural Management and Erosion Losses), a distributed continuous simulation model to simulate daily phosphorus (P) transformations and transport at the catchment scale. CAMEL is a process-oriented mass-balance model that is based on both analytical and numerical approaches. In the model, a catchment is represented using a network of square grid cells each of which is comprised of various storages of water, sediment and P. Most of hydrological processes, soil erosion, sediment transport, and P transformations and transport are described using process-based equations. The P transformations between five P storages (active organic, stable organic, labile, active inorganic, and stable organic) are described using first-order kinetic equations. A comprehensive cascade routing scheme is used to simulate P retention and transport along the channel system. Dissolved P is also transported by groundwater flows, described using a two-dimensional Boussinesq equation. CAMEL simulates both surface and subsurface processes explicitly and therefore is suitable for catchment-scale applications. The distributed, process-oriented structure of CAMEL enables the model to be used for identifying critical source areas of P at the catchment-scale. CAMEL is also computationally efficient, allowing for long-term scale applications.

1. Introduction

The mechanism of phosphorus (P) loss from agricultural land to watercourses involves a series of P transformation and transport processes. P transformations in the soil include decomposition and mineralisation of organic P, immobilisation of labile P and sorption of labile P to/from sediment particles. P dissolved in soil water and P adsorbed to sediment particles can be transported to water bodies by a range of different surface and subsurface pathways. Surface pathways are often strongly associated with sediment transport because P is readily adsorbed to sediment particles. P is most

B. K. Koo et al.

EGU

commonly assumed to be transported predominantly in particulate forms through soil erosion by surface runoff (Walling et al., 1997; Bowes et al., 2003). However, where soil erosion is limited (e.g. as a result of high surface roughness associated with permanent vegetation cover), the majority of P transported by surface runoff may be in dissolved forms (Haygarth and Jarvis, 1997; Heathwaite and Dils, 2000). While surface runoff is an important pathway of P transport, its occurrence is highly variable both in time and space. It has been assumed commonly that P loss through subsurface pathways is small. This may be true for matrix flow as it is unlikely to initiate significant P transport (Heathwaite et al., 2000), However recent studies have reported that preferential flows, through soil macropores or field drains, can be major pathways of P in both particulate and dissolved forms (Gupta et al., 1999; Heathwaite and Dils, 2000; Simard et al., 2000; Chapman et al., 2001; Gardner et al., 2002). In particular, field drains are evidently effective conduits for P export from agricultural catchments (Dils and Heathwaite, 1999). Also, a significant amount of P adsorbed onto colloidal material from slurry or livestock faeces can rapidly move through soil macro-pores (McGechan et al., 2002; McGechan, 2002). Within the river system, P undergoes numerous transformation processes in the course of transport. Important processes related to P transformation within the river system include, amongst others, detachment and deposition of sediment particles, adsorption and desorption of soluble P to/from sediment particles both in suspension and in the river-bed (House et al., 1995). The combination of these processes, in tandem with variations in river flow and other environmental factors, makes the P transport process very complicated.

The significance of each of the P transformation and transport processes varies greatly in space. Thus a small fraction of the catchment area may contribute a large proportion of the P load. These critical source areas (CSAs) are characterised by having high potential to release P into surface or subsurface runoff in conjunction with hydrologic connectivity with streams (Needelman et al., 2001). Because of their high pollution potential, CSAs are of a major concern in catchment management. Gburek and Sharpley (1998) notes that specific P control measures implemented within a

comprehensive management strategy will reduce P losses most effectively only if they are targeted to CSAs. For effective catchment management, therefore, the location of CSAs and the major processes of P transport mechanisms from CSAs, need to be identified.

A mathematical model can play a major role in identifying CSAs of P provided the model structure is appropriate for that purpose. There are a number of continuous simulation models suggested for P transformation and transport processes at the catchment scale. These include HSPF (Bicknell et al., 1997), AnnAGNPS (Cronshey and Theurer, 1998; Theurer and Cronshey, 1998), ANSWERS-2000 (Bouraoui and Dillaha, 2000), SWRRB-WQ (Arnold et al., 1991), SWAT-2000 (Neitsch et al., 2001), ACRU2000 (Campbell et al., 2001), LASCAM (Viney et al., 2000) and INCA-P (Wade et al., 2002). However, most of these models have limitations in identifying CSAs of P. Some models divide a catchment into sub-catchments (e.g. AnnAGNPS, SWRRB-WQ and LASCAM) and others further divide sub-catchments into hydrologic response units (HRUs) or something similar to HRUs (e.g. HSPF, SWAT-2000 and INCA-P). Models using subcatchments as calculation units usually have limitations in identifying CSAs due to their coarse spatial resolutions, although in theory subcatchments can be made as small as one wishes. In those models using HRUs, hydrologic and hydrochemical processes are calculated for individual HRUs, but the calculation results are aggregated to the subcatchment level. This means that HRUs are not connected to each other nor to the stream network and, therefore, transport processes within subcatchments are ignored. This is a somewhat severe limitation given the importance of the connectivity of a source area to the stream network in the transport of sediment-related pollutants, such as P. Moreover, both types of these models have a common problem with calculation units (subcatchments or HRUs) that are an irregular shape and of different sizes. The degree of aggregation for evaluating some parameters (e.g. mean slope of ground surface) varies with the shape and the size of calculation units, and, therefore, certain processes (e.g. sediment transport) cannot be evaluated in a consistent manner across the catchment. Because of these limitations, semi-distributed models may not

A distributed continuous simulation model

B. K. Koo et al.

Title Page

Abstract | Introduction

Conclusions | References

Tables | Figures

◄ | ►|

◄ | ►

Back | Close

Full Screen / Esc

Print Version

Interactive Discussion

EGU

be suitable for identifying CSAs.

In this sense, a distributed approach using square grid cells is more appropriate, but there are few distributed, continuous simulation models that simulate P transformation and transport processes at the catchment scale. ANSWERS-2000 and ACRU2000 are
5 such models that represent a catchment with a network of square grid cells. However, ANSWERS-2000 does not simulate some subsurface processes such as preferential flows through soil macropores and field drains. Therefore, the model may not be suitable for catchments where contribution of such subsurface flows to stream flow is significant. ACRU2000 estimates soil erosion using the modified USLE (Williams,
10 1975). This method does not adequately deal with soils where organic matter contents are greater than 4% (Lilly et al., 2002) and is therefore considered inappropriate for applications (such as in Scotland) where soils with high organic matter contents are common.

The perceived inadequacies of existing methods to address various catchment pro-
15 cesses for identifying CSAs of P in the context of Scottish environment have motivated the development of a new model CAMEL (Chemicals from Agricultural Management and Erosion Losses). This paper presents the theory of the model.

2. Model overview

CAMEL has been developed in an inter-disciplinary project that focused on long-term
20 catchment management in the context of the Water Framework Directive. At the design stage of CAMEL, requirements for the new model were identified in a broad sense:

- To simulate P transformation and transport processes at the catchment scale in the context of the Scottish environment;

- To identify critical source areas (CSAs) of P;

25 - To identify P transport processes through surface and subsurface pathways;

EGU

- – To analyse the long-term effect of land-use management on water quality;

- – To analyse the impact of climate changes on water quality.

CAMEL represents hydrological and hydrochemical processes in a distributed manner using a network of square grid cells. The model simulates daily P transformations using process-oriented equations for each of the grid cells taking into account soil water content and temperature as well as agricultural practices. Transport processes of P in both dissolved and particulate forms are simulated for surface runoff, preferential flows, groundwater flows and river channel flows.

In CAMEL, a grid cell can have a maximum of 8 neighbouring cells any number of which may act as upstream cells but with only one downstream drainage direction. Each of the grid cells represents the corresponding soil-aquifer column of the catchment and has a rectangular stream channel that runs in the middle bisecting the overland surface of the grid cell (Fig. 1). Both sides of the grid cell are inclined toward the channel at the mean slope of the ground surface.

In common with other distributed models, CAMEL requires rather extensive input data:

- – Weather – rainfall, air temperature, dew-point temperature, cloud cover, wind speed and atmospheric pressure at daily time-steps;

- – Topography – ground surface elevation, slope, flow direction, flow accumulation;

- – Land cover – canopy storage capacity of rainfall interception, surface roughness, crop height, root depth, crop coefficient, leaf area index and litter index at each of the growth stages; soil cohesion increase by root reinforcement; livestock excretion rates for cattle and sheep; incorporation rate of plant residue; application rates of fertiliser and manure;

- – Soil – depth; water contents at saturation, field capacity and wilting point, and residual water content; saturated hydraulic conductivity; fractions of sediment par-

ticle size classes, detachability and cohesion of the top soil; volume fraction of the interactive zone around macro pores; equilibrium coefficient for P adsorption;

– Aquifer – depth; water contents at saturation and field capacity, and residual water content; saturated hydraulic conductivity; equilibrium coefficient for P adsorption;

5 – Channel – channel width and depth; channel bed roughness;

The current version of CAMEL provides the following outputs:

– Time-series outputs for any grid cells within the catchment at every time-step;

– "Snapshot" outputs for the entire catchment at specific time-steps and cumulative snapshot outputs for the whole simulation period;

10 – Mass balance outputs of water, sediment and P for the entire catchment at every time-step.

CAMEL is written in an object-oriented language, VB.NET. The model structure is implemented so that each component of the model can be easily modified or extended.

3. Hydrological processes

15 For simulation of hydrological processes, CAMEL uses four water storages – canopy, soil, aquifer and channel (Fig. 2). The aquifer is divided into two layers – the upper layer and the lower layer representing fast-flowing and slow-flowing layers, respectively. Major hydrological processes in and between these storages are described below.

3.1. Rainfall Interception and evapotranspiration

20 When rain falls, a fraction of the rainfall is intercepted and stored in the vegetation canopy. The canopy storage capacity at a given time is assumed to be proportional

to the leaf area index reflecting both seasonal variation of the vegetation canopy (i.e. growth and leaf fall) and agricultural practices (e.g. harvest). Through-fall, i.e. the rainfall that reaches the soil surface, is then estimated by subtracting the amount of rainfall interception from the amount of rainfall.

5   For the estimation of potential evaporation and reference crop transpiration, CAMEL uses two derivatives of the Penman equation suggested by Shuttleworth (1993):

$$E_p = \frac{\delta\,(R_n + A_h)}{\delta + \gamma} + \frac{\gamma}{\delta + \gamma} \cdot \frac{6.43\,(1 + 0.536U_2)\,D}{\lambda} \tag{1}$$

$$E_{rc} = \frac{\delta\,(R_n - G)}{\delta + \gamma\,(1 + 0.33U_2)} + \frac{\gamma}{\delta + \gamma\,(1 + 0.33U_2)} \cdot \frac{900}{T + 275}U_2 D \tag{2}$$

where E_p is potential evaporation rate (mm day^{-1}), E_{rc} is reference crop transpira-
10 tion rate (mm day^{-1}), R_n is net radiation exchange for the free water surface (MJ m^{-2} day^{-1}), A_h is energy advected to the water body (MJ m^{-2} day^{-1}) which is ignored in the model, δ is gradient of saturated vapour pressure over temperature (kPa °C^{-1}), γ is psychrometric constant (kPa °C^{-1}), U_2 is wind speed measured at 2 m above the ground surface (m s^{-1}), D is vapour pressure deficit (kPa), λ is latent heat of vapori-
15 sation of water (MJ kg^{-1}), G is heat conduction into the soil (MJ m^{-2} day^{-1}), and T is daily mean air temperature (°C).

Direct evaporation from the canopy is assumed to take place at the rate of potential evaporation prior to transpiration process. The transpiration rate of a crop is estimated from E_{rc} considering the crop coefficient and soil water stress factor as the following:

20 $$E_c = k_\psi K_{co} E_{rc} \tag{3}$$

where E_c is transpiration rate of a crop (mm day^{-1}), k_ψ is soil water stress factor and K_{co} is potential crop coefficient. The soil water stress factor, k_ψ, is 1.0 when soil water content is greater than the field capacity, but when soil water content falls below the

EGU

field capacity, k_ψ linearly decreases to zero as soil water content reaches the wilting point.

When the leaf area index of a crop is below 1.0, evaporation from the bare soil takes place. The evaporation from the soil surface, E_s, is estimated on an assumption that E_s is proportional to E_p and to a power function of the effective soil saturation:

$$E_s = \begin{cases} 0 & \text{(if } LAI \geq 1) \\ E_p \left(1 - LAI\right) \left(\frac{\theta - \theta_{res}}{\theta_{sat} - \theta_{res}}\right)^m & \text{(if } LAI < 1) \end{cases} \quad (4)$$

where E_s is evaporation from the soil surface (mm day^{-1}), LAI is leaf area index (m^2 m^{-2}), θ is soil water content (m^3 m^{-3}) at a given time, θ_{sat} is saturated soil water content (m^3 m^{-3}), and θ_{res} is residual soil water content (m^3 m^{-3}), m is soil evaporation coefficient.

3.2. Infiltration, saturation and surface runoff

Infiltration of rainfall is represented in CAMEL using the Green-Ampt model (Green and Ampt, 1911) modified by Mein and Larson (1973):

$$f = 1000 k_{eff} \left[1 + \frac{S_f \left(\theta_{sat} - \theta\right)}{F}\right] \quad (5)$$

where, f is maximum infiltration rate (mm h^{-1}), k_{eff} is effective hydraulic conductivity (m h^{-1}), S_f is matric potential of suction at the wetting front (mm), and F is accumulated infiltration (mm). When the rainfall intensity is less than the maximum infiltration rate, all rainfall infiltrates into the soil. When the rainfall intensity is greater than the maximum infiltration rate, a numerical method is used to calculate the accumulated infiltration: f in Eq. (5) is replaced with dF/dt and the integrated finite-difference form of Eq. (5) is iteratively solved for F using a successive substitution approach. Here, for minimising numerical errors, the accumulated infiltration is estimated using daily mean hourly

EGU

rainfall intensity. Any excess of the daily rainfall above the accumulated infiltration contributes to the infiltration-excess surface runoff. When the soil-aquifer column is entirely saturated, the infiltration rate becomes zero and any further rainfall contributes to the infiltration-excess surface runoff. If the soil-aquifer column is fully saturated because of the groundwater table rise, saturation-excess surface runoff is generated.

Surface runoff flows to the stream channel via a rill system. Based on the study of Gilley et al. (1990), it is assumed that one rill exists within every one-metre-wide section of ground surface sloping down to the stream channel. So, an array of rills meets the stream channel at a right angle on both sides of the stream channel. Rill flow rate is assumed to be the same in each rill and the width of rill flows is estimated using a power function of the flow rate as suggested by Gilley et al. (1990):

$$W_r = 1.13 q_r^{0.303} \tag{6}$$

where, W_r is width of rill flows (m) and q_r is flow rate in a rill (m^3 s^{-1}). Note in Eq. (6) that rill flow rate varies over time and, consequently, the rill flow width changes over time. Using the estimated width of rill flow, the rill flow velocity is estimated using the Manning's equation. The model ignores inter-rill flows assuming that all inter-rill flow is drained to the rill system within a daily time-step.

3.3. Preferential flow

In CAMEL, when soil water content exceeds the field capacity, the bottom of the soil layer is assumed to be saturated while the upper part remains at field capacity. This partial saturation creates a perched water table if the genuine groundwater table is not within the soil layer. Whether perched or genuine, if the elevation of the water table is higher than the channel bed, preferential flow through soil macropores is initiated as a Darcian flow. It is assumed that macropores develop only in vegetation-covered areas and that the effective hydraulic conductivity is equal to the standard saturated hydraulic

conductivity times a macroporosity factor:

$$k_{eff} = k_{sat} \cdot A \tag{7}$$

where k_{eff} and k_{sat} are effective and saturated hydraulic conductivity of the soil (m day^{-1}), respectively, and A is the macroporosity factor. The macroporosity factor is estimated for undisturbed soils (Rawls et al., 1989):

$$A = \exp\left(2.82 - 0.099 S\% + 1.94 \delta_b\right) \tag{8}$$

and for disturbed soils (Brakensiek and Rawls, 1988):

$$A = \exp\left(0.96 - 0.032 S\% + 0.04 C\% - 0.032 \delta_b\right) \tag{9}$$

where $S\%$ and $C\%$ are volume percent of sand and clay (%), respectively, and δ_b is bulk density of the soil (g cm^{-3}). The maximum value of macroporosity factor is restricted to 18 as suggested by Rawls et al. (1989) and it is assumed that uncovered areas have no macropores (i.e. $A=1$).

Another form of preferential flow represented in the model is field drainage. In many agricultural fields in the UK, field drains have been installed to lower the water table in the soil. In such systems, field drains transport soil water directly to the stream channel. If the water table is above the drain tiles, drain flow is initiated. Estimation of the field drain flow is based on the drainage equation by Hooghoudt (1940):

$$Q_{fd} = \frac{4 k_{eff} \Delta h \left(2 d_{eq} + \Delta h\right)}{\Delta l^2} \Delta x^2 \tag{10}$$

where Q_{fd} is preferential flow through field drains (m^3 day^{-1}), d_{eq} is equivalent depth (m), Δx is cell size (m), and Δl is field drain spacing (m).

3.4. Aquifer recharge

Aquifer recharge in the model occurs only when soil water content is higher than the field capacity. The amount of water flowing through the soil layer to the aquifer is

A distributed continuous simulation model

B. K. Koo et al.

EGU

estimated using a storage routing method similar to that in SWAT-2000 (Neitsch et al., 2001). For taking into account the effect of varying unsaturated hydraulic conductivity, calculations are carried out for individual 0.1% slices of soil water content above the field capacity:

$$q_{sa} = 0.001 \cdot V_{ss} \left[1 - \exp\left(-\Delta t / t_T \right) \right] \tag{11}$$

where q_{sa} is amount of water flow from the soil to the aquifer (m^3) calculated for individual 0.1% soil water content, V_{ss} is volume of the soil layer (m^3), Δt is time step (day), and t_T is travel time of the recharge flow (day). Here, t_T is evaluated by dividing mean flow distance by unsaturated hydraulic conductivity (Eq. 12) that is estimated using the Averjanov equation (Averjanov, 1950) (Eq. 13):

$$t_T = \frac{1}{2} \frac{d_{soil}}{k_{unsat}} \tag{12}$$

$$k_{unsat} = k_{sat} \left(\frac{\theta - \theta_{res}}{\theta_{sat} - \theta_{res}} \right)^n \tag{13}$$

where d_{soil} is depth of the soil layer (m), k_{unsat} is unsaturated hydraulic conductivity of the soil layer (m day^{-1}), and n is Averjanov's exponent. Estimation of q_{sa} using Eq. (11) is repeated for each 0.1 % slice of soil water content above the field capacity and all q_{sa} are added together to give the total amount. The total amount of water flow from the soil to the aquifer is then limited by the percolation rate of the aquifer:

$$Q_{sa} = \min \left(\frac{\sum q_{sa}}{\Delta t}, K_{sat} \Delta x^2 \right) \tag{14}$$

where Q_{sa} is total water flow from the soil to the aquifer (m^3 day^{-1}) and K_{sat} is saturated hydraulic conductivity of the fast-flowing aquifer layer (m day^{-1}). Also, groundwater recharge flux within an aquifer column is estimated using an approach similar to the presented above.

EGU

3.5. Channel routing

For routing of the channel water, the spatially distributed unit hydrograph approach proposed by Maidment (1993) was adopted in CAMEL with modifications. Based on an assumption that mean flow velocity is spatially variable but time- and discharge-invariant, isochrones of the flow travel time to the catchment outlet are determined for each of the grid cells. The amount of channel water leaving a given isochrone area in a time step (ordinates of a unit hydrograph) constitutes a unit hydrograph at the catchment outlet. Individual unit hydrograph ordinates from each of the isochrone areas are then linearly superposed to give total discharge at the catchment outlet (Fig. 3). The mean flow velocity for each grid cell is estimated using the Manning's equation with the mean channel water depth that is specified by the user as a fraction of the channel width based on the observed flow data. It should be noted that the mean flow velocity estimated this way is used solely for calculating the mean travel time of channel water flow and that the real flow velocity is estimated at every time step using the results of channel routing. By applying this procedure not only to the catchment outlet but also to all other grid cells, channel discharge variables are estimated at every grid cell within the catchment. This approach may not be appropriate for simulating propagation of flood waves at a fine resolution of time, but it is considered to be reasonably accurate for daily time-step simulations.

3.6. Aquifer-channel interaction

The aquifer interacts with the stream channel through the channel bed whenever there is a difference in water heads between the groundwater table and the channel water level. When the groundwater table is higher than the channel water level, groundwater flows into the channel, and vice versa. Both flows are assumed to be Darcian flows and are estimated using a saturated hydraulic conductivity corresponding to the fast-flowing aquifer layer.

3.7. Groundwater flow

In the model, groundwater flows are described as horizontal flows between grid cells and the vertical flow component is ignored. Based on the widely-used assumption that groundwater flow follows the Darcian law, the groundwater flow is described by the following two-dimensional Boussinesq equation:

$$S\frac{\partial h}{\partial t} = \frac{\partial}{\partial x}\left(K_{sat}H\frac{\partial h}{\partial x}\right) + \frac{\partial}{\partial y}\left(K_{sat}H\frac{\partial h}{\partial y}\right) \tag{15}$$

where S is the storage coefficient of the aquifer (m m^{-1}), t is time (day), h is elevation of groundwater table (m), and H is saturated thickness of the aquifer (m). Expanding the terms in Eq. (15) to finite-difference analogues gives a non-linear equation for each of the grid cells with groundwater table elevation, h, as the dependent variable. The system of equations for all grid cells is then solved iteratively using a successive over-relaxation method. This approach is valid providing the groundwater flow velocity ($=K_{sat}\Delta h\Delta x^{-1}$) is less than the grid cell size divided by a daily time-step (Δx day^{-1}).

4. Soil erosion and transport processes

Sediment erosion and transport processes take place both on the land and within the channel. Equations for the soil erosion and transport component of CAMEL have been largely taken from the EUROSEM model (Morgan et al., 1998). For simulating the effect of sediment supply, an approach based on the sediment transport capacity is applied using two sediment storages – overland sediment storage and channel sediment storage (Fig. 4). Each of these storages consists of four sub-storages of clay, silt, fine sand and coarse sand. For simplicity, a representative value of particle size (effective diameters) is used for each of the particle size classes: 1 μm for clay; 10 μm for silt; 100 μm for fine sand; and 1000 μm for coarse sand.

A distributed continuous simulation model

B. K. Koo et al.

Title Page

Abstract	Introduction
Conclusions	References
Tables	Figures

◄	►
◄	►
Back	Close

Full Screen / Esc

Print Version

Interactive Discussion

EGU

4.1. Splash detachment

During a rainfall event, sediment particles on the soil surface are detached by raindrop impacts. This splash detachment by rain drops is related to the kinetic energy of rainfall and is estimated in CAMEL for both direct rainfall and leaf drainage from the canopy. The kinetic energy of rainfall reaching the ground surface can be described by the following (Brandt, 1989, 1990):

$$KE_r = \max\left(8.95 + 8.44 \log \iota, 0\right) \cdot R \tag{16}$$

$$KE_l = \max\left(15.8\sqrt{H_c} - 5.87, 0\right) \cdot (R - I_c) \tag{17}$$

where KE_r is kinetic energy of direct rainfall (J m^{-2}), KE_l is kinetic energy of leaf drainage from the canopy (J m^{-2}), ι is rainfall intensity (mm h^{-1}), R is daily rainfall (mm), I_c is canopy interception (mm), and H_c is canopy height (m). Note that KE_l in Eq. (17) becomes zero if the canopy height is less than 14 cm. The total kinetic energy is estimated by taking into account the ground surface condition. The splash detachment is calculated for each of the particle size classes (Morgan et al., 1998) by:

$$SD_i = 10\eta \left[KE_r \left(1 - \lambda_c\right) + KE_l \lambda_c\right] \exp\left(-b d_{sw}\right) \varsigma_i \tag{18}$$

where SD is splash detachment by rain drop impact (kg ha^{-1}), η is soil detachability index (g J^{-1}), λ_c is a fraction of ground surface covered by plant canopy, b is rain drop impact attenuation coefficient, d_{sw} is depth of overland surface water (mm), ς is fraction of a given particle size class in the top soil, and i is subscript for particle size classes. It is assumed that sediment particles mobilised by splash detachment constitute the initial sediment concentration in the surface runoff.

4.2. Flow detachment

Sediment detachment by rill flows is simulated according to the erosion–deposition theory proposed by Smith et al. (1995). The sediment concentration at the transport

EGU

capacity represents the sediment concentration at which the rate of erosion and the accompanying rate of deposition are in balance. The equation for sediment erosion and deposition during rill flow is expressed in terms of settling velocity and transport capacity (Smith et al., 1995):

$$FD_i = \varepsilon_d v_i \left(TC_i - C_i\right) W_r \tag{19}$$

where FD is sediment detachment by the rill flow (kg m^{-1} s^{-1}), ε_d is detachment efficiency coefficient, v is settling velocity of sediment particles (m s^{-1}), TC is sediment transport capacity of the rill flow (kg m^{-3}), and C is initial sediment concentration in the rill flow (kg m^{-3}). The initial sediment concentration is estimated by dividing the amount of splash detachment by the amount of surface runoff. The settling velocity of sediment particles is estimated using Stokes' law, assuming constant density and viscosity of water.

The sediment transport capacity of the rill flow at a given point is the maximum net erosion potential and is estimated as the following (Govers, 1990; Morgan et al., 1998):

$$TC_i = \alpha_i \rho \left(\omega - \varpi_i\right)^{\beta_i} \tag{20}$$

$$\omega = s \cdot \bar{u} \tag{21}$$

$$\alpha_i = \left(\frac{\phi_i + 5}{0.32}\right)^{-0.6} \tag{22}$$

$$\beta_i = \left(\frac{\phi_i + 5}{300}\right)^{0.25} \tag{23}$$

where α and β are experimentally-determined coefficients, ρ is density of sediment particles (=2650 kg m^{-3}), ω is unit stream power (cm s^{-1}), ϖ is critical value of unit stream power (cm s^{-1}), s is energy slope of water, ω is mean flow velocity (cm s^{-1}), and ϕ is median particle size (μm). If the sediment transport capacity is greater than the

Title Page

Abstract | Introduction

Conclusions | References

Tables | Figures

|◄ | ►|

◄ | ►

Back | Close

Full Screen / Esc

Print Version

Interactive Discussion

EGU

initial sediment concentration, more sediment particles may be detached (flow detachment) and transported to the channel. If the sediment transport capacity is less than the initial sediment concentration, however, a part or all of the detached sediment may be deposited and added to the overland sediment storage. Govers (1990) introduced the critical unit stream power, ϖ, and suggested a value of 0.4 cm s^{-1}, but his study covers only a limited range of particle sizes from coarse silt to coarse sand. Therefore the suggested value may not be valid for clay and fine silt. In CAMEL, the value of ϖ for each of the particle size classes can be adjusted by the user.

The detachment efficiency coefficient, ε_d, in Eq. (19) is used to represent the effect of cohesive soil material on sediment detachment and is defined as a function of the cohesion of wet soil (Rauws and Govers, 1988):

$$\varepsilon_d = \frac{1}{0.89 + 0.56\zeta} \tag{24}$$

where ζ is cohesion of wet soil (kPa). By definition, ε_d takes a value of 1 when the sediment transport capacity is less than the initial concentration (i.e. when net deposition occurs).

4.3. Sediment transport to the channel

The amount of sediment transported to the channel by rill flow depends on the transport capacity of the rill flow and the overland sediment storage. When the transport capacity is greater than the initial concentration, flow detachment takes place but its amount is limited to the overland sediment storage. If the transport capacity is less than the initial concentration, excess sediment is deposited on the land and no flow detachment takes place. The overland sediment storage thus represents the amount of disaggregated sediment particles on the ground surface. To reflect soil aggregation processes, the size of overland sediment storage is assumed to exponentially decrease over time.

Transport of sediment particles by preferential flows through soil macropores and field drains is not included in the model due to the complexity of the transport process.

EGU

4.4. Channel routing – sediment

Sediment transported to the channel through the rill system is added to the channel sediment storage and is transported downstream by channel flows. A comprehensive cascade routing scheme has been developed to simulate sediment detachment and deposition processes along the channel network. The channel sediment budgets are calculated first for first-order cells with no upstream cells. The amount of sediment leaving each of the first-order cells is then calculated and routed downstream cell by cell taking into account the isochrones in the course of the downstream transport. Sediment transport processes in the channel are estimated using the same erosion-deposition theory applied to the rill flow in Eq. (19), but the sediment cohesion effect is ignored ($\varepsilon_d=1$) on the assumption that sediment particles on the channel bed are loose. As sediment transport processes are estimated for each of four particle size classes, the composition of the channel bed sediment may vary according to the transport capacity of the channel flow at a given time and space.

5. P transformation processes

P transformation processes in CAMEL are simulated for organic and inorganic P storages in the soil, aquifer and channel (Fig. 5). For simplification, organic P storages in the aquifer and the channel are ignored. Organic P in the soil is divided into two storages: the active organic P storage (P_{AO}) and the stable organic P storage (P_{SO}). P_{AO} consists of P in undecomposed plant residues, livestock excretion, manure and microbes, whereas P_{SO} is composed of P in stable organic matter i.e. humus. Inorganic P is divided into labile P (P_{LB}), active inorganic P (P_{AI}) and stable inorganic P (P_{SI}) storages. P_{LB} is in rapid equilibrium with P_{AI} which in return is in slow equilibrium with P_{SI}. When inorganic fertiliser P is added, it rapidly equilibrates between P_{LB} and P_{AI}. The slow reaction between P_{AI} and P_{SI} then follows. It is assumed P_{SI} is four times larger than P_{AI}. In the aquifer and the channel, only inorganic P storages (P_{LB}, P_{AI} and P_{SI})

are assumed and, therefore, P adsorption and desorption are the only transformation processes simulated in the model.

It is assumed that vertical distribution of P in the soil reaches its maximum at the soil surface and exponentially decreases with depth. Unlike in the soil, P in the aquifer and the channel is assumed to be completely mixed within each of the storages.

5.1. P transformations in the soil

All P transformation rates are estimated using first-order kinetic equations taking into account the effect of soil water content and temperature.

The decomposition rate of active organic matter is assumed to be constant, regardless of the fraction of fresh organic matter remaining since the last incorporation into the soil. It is also assumed that the decomposition rate is not limited by either the C/N or C/P ratio:

$$\xi_d = k_d k_{TB} k_\theta P_{AO} \tag{25}$$

where ξ_d is active organic P decomposition rate (kg-P ha^{-1} day^{-1}), k_d is rate coefficient for active organic matter decomposition (day^{-1}), k_{TB} is temperature adjustment factor for biochemical processes, k_θ is soil water adjustment factor, and P_{AO} is active organic P in the soil (kg-P ha^{-1}). When active organic P is decomposed, it is assumed that 80% of the decomposed P undergoes mineralisation and the remaining 20% is incorporated into the stable organic P storage (P_{SO}). So the total mineralisation rate of P is estimated as the following:

$$\xi_m = 0.8\xi_d + k_h k_{TB} k_\theta P_{SO} \tag{26}$$

where ξ_m is P mineralisation rate (kg-P ha^{-1} day^{-1}), k_h is rate coefficient for humus mineralisation (day^{-1}), P_{SO} is stable organic P in the soil (kg-P ha^{-1}). Mineralised P is added to the labile P storage and there is a reverse process that incorporates labile P back to organic P. However, this immobilisation rate of P is only a very small fraction of the decomposition rate (Jones et al., 1984) and therefore is ignored in the model.

EGU

A distributed continuous simulation model

B. K. Koo et al.

Print Version

Interactive Discussion

Adsorption of P from the solution to the surface of sediment particles is simulated in two separate processes. When a gradient of P concentrations exists between inorganic P storages, a rapid equilibrium is initially reached between P_{LB} and P_{AI} and then a subsequent slow reaction takes place between P_{AI} and P_{SI}. The rapid adsorption rate of P from the labile P storage to the active inorganic P storage is estimated using Eq. (27):

$$\xi_{ra} = k_{ra} k_{TS} k_{\theta} \left(\sigma_{ra} P_{LB} - P_{AI} \right) \tag{27}$$

where ξ_{ra} is rapid adsorption rate of P from P_{LB} to P_{AI} (kg-P ha^{-1} day^{-1}), k_{ra} is rate coefficient for rapid adsorption of P from P_{LB} to P_{AI} (day^{-1}), k_{TS} is temperature adjustment factor for sorption (can exceed 1.0), P_{LB} is labile P storage (kg-P ha^{-1}), P_{AI} is active inorganic P storage (kg-P ha^{-1}), and σ_{ra} is equilibrium coefficient for rapid adsorption.

The slow adsorption rate of P from the active inorganic P storage to the stable inorganic P storage is estimated by assuming that P_{SI} is four times larger than P_{AI} in equilibrium:

$$\xi_{sa} = k_{sa} \left(4 P_{AI} - P_{SI} \right) \tag{28}$$

where ξ_{sa} is slow adsorption rate of P from P_{AI} to P_{SI} (kg-P ha^{-1} day^{-1}), k_{sa} is rate coefficient for slow adsorption of P from P_{AI} to P_{SI} (day^{-1}), and P_{SI} is stable inorganic P storage in the soil (kg-P ha^{-1}).

From the P transformation processes defined in Eqs. (25) to (28), the changes in the five P storages are estimated at every time step using a fourth-order Runge-Kutta method for simultaneous solution of the equations.

5.2. Plant uptake

Uptake of P (mainly in the form of $H_2PO_4^-$) by plant roots is assumed to follow Michaelis-Menten kinetics (Barber, 1980) and is limited by soil water availability:

$$P_{up} = U_{max}\mu \cdot \frac{C_{DP(rz)}}{M\mu + C_{DP(rz)}} \cdot k_\psi \qquad (29)$$

where P_{up} is P uptake rate by a given plant (kg-P ha^{-1} day^{-1}), U_{max} is maximum rate of P uptake by the given plant (kg-P ha^{-1} day^{-1}), μ is a ratio of potential crop coefficient for a given day to the maximum crop coefficient ($=K_{co}/K_{co(max)}$), $C_{DP(rz)}$ is concentration of dissolved P in the root zone (kg-P m^{-3}), and M is Michaelis-Menten's half-saturation constant of dissolved P concentration for the given plant (kg-P m^{-3}). Note in Eq. (29) that U_{max} and M are multiplied by μ to reflect the seasonal variation of crop growth and hence P demand. The soil water stress factor (k_ψ) is applied to limit the P uptake rate according to soil water availability. There is no limitation when the soil water content exceeds the field capacity, but P uptake decreases linearly as the soil water content decreases from field capacity to wilting point and no uptake occurs when the soil water content is below the wilting point. Thus, Eq. (29) reflects both the P demand and availability in the root zone.

5.3. Factors affecting P transformations

P transformation processes in the model are affected by two environmental factors – soil water content and soil temperature. The effect of soil water content on organic matter decomposition and mineralisation is estimated using a segmented linear function: the soil water adjustment factor (k_θ) is zero when there is no soil water, then increases linearly with soil water content to its maximum (= 1) when the soil water content is at field capacity. The maximum value is maintained until the soil water content is at the mid-point between field capacity and saturation and then decreases to 0.6 when the soil is fully saturated.

A distributed continuous simulation model

B. K. Koo et al.

Temperature influences the rates of all of the P transformation processes. The effect of temperature on rates of organic matter decomposition and mineralisation, which are driven by microbial activities, is estimated using the soil respiration rate equation proposed by Lloyd and Taylor (1994):

$$k_{TB} = \exp\left(4.34 - \frac{308.56}{T' + 46.02}\right) \tag{30}$$

where T' is daily mean soil temperature (˚C). Another temperature adjustment factor is used to estimate the effect of temperature on P sorption (Jones et al., 1984):

$$k_{TS} = \exp\left(0.115T' - 2.88\right) \tag{31}$$

Note that k_{TB} and k_{TS} are equal to unity when the soil temperature is 25 ˚C.

To evaluate the temperature adjustment factors in Eqs. (30) and (31), the mean daily soil temperature is estimated using the approach of Kang et al. (2000) in which the effects of ground litter as well as leaves are accounted for:

$$T'_t = T'_{t-1} + \left(T_t - T'_{t-1}\right) \cdot \exp\left[-z\left(\frac{\pi}{\kappa p}\right)^{1/2}\right] \cdot \exp\left(k_e LL_t\right) \tag{32}$$

$$LL_t = \begin{cases} LAI_t + LIT_t & \left(\text{if } T_t > T'_{t-1}\right) \\ LIT_t & \left(\text{if } T_t \leq T'_{t-1}\right) \end{cases} \tag{33}$$

where z is soil depth (m), κ is thermal diffusivity of the soil (cm^2 s^{-1}), p is period of diurnal temperature variation (=86 400 s), k_e is extinction coefficient for solar radiation interception through the canopy, LL is combined index of leaf area and ground litter (m^2 m^{-2}), LIT is LAI equivalent of ground litter (m^2 m^{-2}), and t and $t-1$ are subscripts for daily time-step (day). In the model, for simplicity, soil temperature at a fixed depth of 10 cm is estimated and used. Thermal diffusivity of soil varies in a range depending on the soil texture, organic matter and soil water content. However, according to Kang et al. (2000), soil temperature in Eq. (32) is not very sensitive to thermal diffusivity,

but is very sensitive to *LL*. The model uses a constant value for the extinction coefficient for solar radiation interception (k_e=0.45) and for the thermal diffusivity of the soil (κ=5×10^{-7} m^2 s^{-1}).

6. P transport processes

In CAMEL, P transport processes are simulated for both sediment-bound P (particulate P) and dissolved P. The amount of particulate P transported with sediment particles is estimated using P adsorption capacity of each of the sediment particle size classes and the transport of dissolved P is estimated using a transfer function. Dissolved P here refers to inorganic P only and the transport of dissolved organic P is not simulated in the model.

6.1. Transport of particulate P by surface runoff

For estimating transport of particulate P by surface runoff from overland to channel, it is assumed that only particulate P in the top 1 cm of the soil can be transported. The amount of P transported in particulate form by surface runoff is estimated for each particle size class using Eq. (34):

$$PP_{sr} = S_{sr} \cdot C_{PP(top)} \cdot \varepsilon_p \tag{34}$$

where PP_{sr} is amount of particulate P transported from the soil to the channel (kg-P ha^{-1}), S_{sr} is sediment transported to the channel by surface runoff (kg ha^{-1}), $C_{PP(top)}$ is concentration of particulate P in the top 1 cm of the soil (kg-P kg^{-1}), and ε_P is enrichment ratio of P. $C_{PP(top)}$ is estimated based on top soil texture, vertical distribution of P, and P adsorption capacity of sediment particles. The enrichment ratio, ε_p, is defined as the concentration of P in the eroded sediment divided by the P concentration in the soil. The enrichment ratio of P in sediment decreases markedly with the amount

of eroded sediment and a logarithmic relationship suggested by Menzel (1980) is used in the model:

$$\varepsilon_p = \exp(2 - 0.2 \ln S_{sr}) \tag{35}$$

Transport of particulate P by preferential flows through soil macropores and field drains is ignored in the model.

6.2. Transport of dissolved P in the soil

Dissolved P is transported to the channel by surface runoff and preferential flows, and it is also transported to the aquifer by recharge flows. As surface runoff flows over the top soil, water interacts with the top soil, transporting some of the dissolved P in pore waters. In the model, this process is conceptualised using a transfer function that estimates the proportion of dissolved P transported from the soil pore water to the channel by surface runoff. It is assumed that surface runoff interacts with the top 1 cm of the soil. The amount of dissolved P transported by surface runoff is estimated by the following:

$$DP_{sr} = P_{LB(top)} \cdot \Pi_{sr} \tag{36}$$

$$\Pi_{sr} = 1 - \exp\left(-\frac{Q_{sr}}{\Omega_{sr}}\right) \tag{37}$$

where DP_{sr} is amount of dissolved P transported from the top soil to the channel by surface runoff (kg-P ha^{-1}), $P_{LB(top)}$ is labile P in the top 1 cm of the soil (kg-P ha^{-1}), Π_{sr} is a transfer function for the dissolved P transported by surface runoff, Q_{sr} is surface runoff expressed in water depth (m), and Ω_{sr} is the amount of surface runoff when 63% of dissolved P is transported (m). As illustrated in Fig. 6, the transfer function Π in Eq. (37) takes an exponential rise-to-maximum form varying from 0 to 1 according to the ratio of Q to Ω. When Q is equal to Ω, 63% of dissolved P in the soil is transported. The rationale behind this transfer function is that the amount of dissolved P transported

1382

EGU

by unit water flow decreases as water flow increases. For a given Q, a larger Ω means less transport of dissolved P and vice versa.

Preferential flows through macropores and field drains are an important hydrologic pathway that may transport a significant amount of dissolved P. When water flows
through macropores, dissolved P in pore waters adjacent to the flow pathway is transferred to the flowing water by advection and diffusion. Preferential flows are a quick transport system, and the amount of dissolved P that is transported is limited by the interaction between the flowing water and pore waters. In the model, movement of dissolved P from pore waters to the flowing water takes place at 'interactive zones' which
represent interactive pores of the soil around flow pathways. The amount of dissolved P transported by field drain flows is estimated by applying a transfer function to the amount of dissolved P in the interactive zone:

$$DP_{fd} = P_{LB(fd)} \cdot \Pi_{fd} \tag{38}$$

where DP_{fd} is amount of dissolved P transported from the soil to the channel by field
drain flows (kg-P ha^{-1}), $P_{LB(fd)}$ is labile P in the interactive zone between water table and field drains (kg-P ha^{-1}), Π_{fd} is transfer function for dissolved P transported by field drain flows, similarly defined as in Eq. (37).

Similarly, the amounts of dissolved P transported through soil macropores to the channel and to the aquifer are estimated by the following:

$$DP_{mp} = P_{LB(mp)} \cdot \Pi_{mp} \tag{39}$$

$$DP_{sa} = P_{LB(sa)} \cdot \Pi_{sa} \tag{40}$$

where DP_{mp} is amount of dissolved P transported from the soil to the channel by macropore flows (kg-P ha^{-1}), DP_{sa} is amount of dissolved P transported from the soil to the aquifer by macropore flows (kg-P ha^{-1}), $P_{LB(mp)}$ is labile P in the interactive
zone below water table (kg-P ha^{-1}), $P_{LB(sa)}$ is labile P in the soil below water table

(kg-P ha^{-1}), and Π_{mp} and Π_{sa} are transfer functions for dissolved P transported by macropore flow and aquifer recharge flow, respectively.

6.3. Transformations and transport of dissolved P in the aquifer

P transformation processes in the aquifer (fast and slow sorption) are estimated using equations similar to Eqs. (27) and (28) based on an assumption that groundwater is completely mixed and that the groundwater temperature is constant. Dissolved P in the aquifer can be transported to the soil by a rise in the groundwater table, to/from the channel by channel-aquifer interaction flows, or to/from the aquifer of neighbouring cells according to water head differences. The amount of dissolved P transported is estimated by multiplying the mean concentration of dissolved P with the corresponding groundwater flux.

6.4. Transformations and transport of P in the channel

Transport of P along the channel network is calculated using the same approach used for channel routing of sediment particles. P transformation processes (fast and slow sorption) are first estimated for first-order cells and then both particulate and dissolved P are transported to the downstream channel where P transformations are estimated taking account of all upstream inputs. Through this comprehensive cascade routing scheme, P transformations and transport are simulated cell by cell all the way down to the catchment outlet.

In-stream P transformation processes are estimated using equations similar to Eqs. (27) and (28), based on the assumption that the channel water is completely mixed and that the channel water temperature is the same as the soil temperature. The P adsorption capacity of the channel bed is determined by particle size distributions of the channel bed sediment storage.

The amount of particulate P transported by channel flows is estimated for each of the particle size classes by multiplying the amount of sediment transported downstream

with the concentration of particulate P in the channel bed sediment storage:

$$PP_{ch} = S_{ch} \cdot C_{PP(ch)} \qquad (41)$$

where PP_{ch} is amount of particulate P transported by downstream channel flows (kg-P), S_{ch} is sediment transported to downstream by channel flows (kg), and $C_{PP(ch)}$ is concentration of particulate P in the channel bed sediment storage (kg-P kg^{-1}). The value of $C_{PP(ch)}$ is estimated using the composition of the channel bed sediment storage and the P adsorption capacity of sediment particles.

As complete mixing is assumed in the channel, the amount of dissolved P transported downstream is proportional to the ratio of downstream water discharge to the total amount of interactive water in the channel:

$$DP_{ch} = P_{LB(ch)} \frac{Q_{ch}}{Q_{ch} + IW_{ch}} \qquad (42)$$

where DP_{ch} is amount of dissolved P transported to the downstream by channel flows (kg-P ha^{-1}), $P_{LB(ch)}$ is labile P in the channel (kg-P ha^{-1}), Q_{ch} is downstream channel water discharge (m^3), IW_{ch} is interstitial water in the channel bed which consists of water in the channel bed sediment storage and in the top 1 cm of the firm channel bed (m^3). The interstitial water in the top 1 cm of the firm channel bed is introduced here to prevent all of the dissolved P from being transported downstream when the channel bed has no loose sediment storage.

7. Discussion

7.1. Suitability of CAMEL for identifying CSAs of P

There are several essential requirements for a catchment model to be able to identify CSAs of P at the catchment scale. Firstly, the catchment model should be spatially-distributed so that variations of P-related processes are simulated across the catchment. CAMEL is fully-distributed in horizontal dimensions, but it is not fully-distributed

A distributed continuous simulation model

B. K. Koo et al.

Title Page

Abstract	Introduction
Conclusions	References
Tables	Figures

◄◄   ►►

◄   ►

Back   Close

Full Screen / Esc

Print Version

Interactive Discussion

EGU

A distributed continuous simulation model

B. K. Koo et al.

Print Version

Interactive Discussion

EGU

vertically, having only one soil layer and two aquifer layers. However, P transport by surface runoff, which is one of the most significant mechanisms of P transport in many areas, is estimated using P pools in the top 1 cm of the soil layer. Thus, although the model is not fully-distributed vertically, the P processes are simulated appropriately.

5   Secondly, both surface and subsurface processes should be simulated to take into account the various transport processes of particulate P and dissolved P. In CAMEL, surface and subsurface hydrological processes are explicitly represented, as are P transport processes. Particulate P is transported only by surface runoff but dissolved P can be transported by surface runoff, preferential flows, groundwater recharge flux,

10   and groundwater flows.

Thirdly, the fate of P during transport along a stream channel network should be simulated. CAMEL has a comprehensive cell-by-cell cascade routing scheme for simulating the fate of sediment particles and P along the stream channel network. Thus CAMEL can simulate deposition and re-suspension of particulate P, and adsorption

15   and desorption of dissolved P. These together define the P retention characteristics over time and space.

Thus, CAMEL satisfies the requirements to a reasonable degree and should be appropriate for identifying CSAs of P at the catchment scale.

7.2.   Other potential application areas

20   CAMEL can be used for other applications as well as for identifying CSAs. As a distributed process-oriented model, it can be used for estimating land use change impacts on water quality. Land use changes (e.g. afforestation or deforestation) in parts of a catchment can be represented in the model by assigning new land covers to the corresponding grid cells. Changed values of land cover related parameters (e.g. surface

25   roughness, LAI, fertiliser application rate, etc.) in process-oriented equations will be translated into changes in the simulated water flow and water quality. Similarly, CAMEL can also evaluate the effectiveness of certain types of BMPs (best management practices) that may be implemented only in parts of a catchment.

Using a comprehensive cascade channel routing scheme, CAMEL simulates detachment, deposition and re-suspension of sediment particles for four particle-size classes. Although the model cannot take account of in-stream heterogeneity within a grid cell, CAMEL simulates the distribution of sediment particles across the whole stream channel network at every daily time-step. Thus, this capability of the model to simulate sediment distributions over space and time can be useful for certain ecological studies regarding sediment-related stream habitats.

CAMEL also takes into account the effects of soil water content and soil temperature on P transformation processes. Thus, the model can evaluate, to a degree, potential impacts of climate change on P dynamics in soil and water.

Although it simulates both surface and subsurface processes in a distributed manner, CAMEL sparingly employs iterative numerical approaches. Thus, the computing power required for CAMEL simulations is relatively low, and therefore the model can be used for long-term simulations.

7.3. Limitations of CAMEL

CAMEL has some limitations in its representation of hydrological and hydrochemical processes, which stem from the structure of the model. The most significant limitations are considered to be:

– CAMEL has only one soil layer and therefore the state variables such as soil water content need to be aggregated for the whole soil column. This may be reasonable for shallow soils, but may not be so for deep soils.

– As the model runs at daily time-steps, state variables are estimated using daily mean values. For estimating slow/steady-processes (e.g. aquifer recharge), daily mean values are reasonable. But for fast/ephemeral-processes (e.g. infiltration-excess runoff), daily mean values may not be appropriate and this could be a major limitation. For example, CAMEL estimates the accumulated infiltration using an hourly rainfall intensity derived from the daily mean. This is likely to sub-

stantially underestimate the real hourly rainfall intensity during storm events. This means that the model is likely to overestimate the accumulated infiltration and consequently underestimate infiltration excess and sediment transport capacity of the surface runoff. This limitation of the model could be alleviated by using rainfall duration data to estimate hourly rainfall intensities. However, this is not included in the current version of the model.

– The current version of the model has no snow component and cannot simulate snow melting events.

– The channel routing components of the model does not allow for lakes or reservoirs.

– In the model, inorganic P is transported in either particulate or dissolved forms, but no transport of organic P is taken into consideration. This is reasonable for intensive agricultural areas where a large amount of inorganic P fertilisers are applied on a regular basis. However, it may not be appropriate for non-agricultural areas or intensive livestock farming areas where the transport of organic P is significant.

– CAMEL has no biological components for in-stream P dynamics and thus cannot simulate decomposition and mineralisation of organic materials or uptake of P by phytoplankton and algae;

The authors hope that these limitations of CAMEL will be addressed in future versions of the model.

8. Conclusions

Phosphorus (P) transformation and transport processes vary greatly in time and space. For effective implementation of P control measures in a catchment, it is of utmost importance to identify critical source areas (CSAs) of P and major P transport processes

from CSAs. A mathematical model can be a useful tool for identifying CSAs of P if the model structure is appropriate.

A distributed continuous simulation model, CAMEL (Chemicals from Agricultural Management and Erosion Losses), has been developed for simulating daily transport of water, sediment and P at the catchment scale. CAMEL describes a catchment using a network of square grid cells that represent corresponding soil-aquifer columns. Every grid cell consists of various storages of water (canopy, soil, aquifer and channel water), sediment (overland and channel-bed sediment) and P (active organic, stable organic, labile, active inorganic and stable inorganic P), and hydrological and hydrochemical processes are described as movements of mass between these storages. With a network of self-contained cells and comprehensive routing schemes, CAMEL is able to simulate both surface and subsurface processes. Although a few conceptual approaches are used, most of the hydrological and hydrochemical processes in the model are represented using process-based equations.

The distributed, process-oriented structure of CAMEL enables the model to be used for identifying CSAs of P at the catchment scale. With sparingly employed iterative numerical approaches, CAMEL requires a relatively low cost of computing power, which allows for long-term scale applications such as evaluating climate change impacts on water quality. The model has been designed to suit the Scottish environment, but is appropriate for application elsewhere in the temperate region.

Notation

α, β experimentally-determined coefficients to estimate sediment transport capacity (dimensionless)

γ psychrometric constant (kPa $°C^{-1}$)

δ gradient of saturated vapour pressure over temperature (kPa $°C^{-1}$)

δ_b bulk density of the soil (g cm^{-3})

ε_d detachment efficiency coefficient (dimensionless)

ε_P	enrichment ratio of P (dimensionless)
ζ	cohesion of wet soil (kPa)
η	soil detachability index (g J^{-1})
θ	soil water content (m^3 m^{-3})
θ_{res}	residual soil water content (m^3 m^{-3})
θ_{sat}	saturated soil water content (m^3 m^{-3})
ι	rainfall intensity (mm h^{-1})
κ	thermal diffusivity of the soil (cm^2 s^{-1})
λ	latent heat of vaporisation of water (MJ kg^{-1})
λ_c	fraction of ground surface covered by plant canopy (dimensionless)
μ	ratio of potential crop coefficient for a given day to the maximum crop coefficient (=$K_{co}/K_{co(\max)}$)
v	settling velocity of sediment particles (m s^{-1})
ξ_d	active organic P decomposition rate (kg-P ha^{-1} day^{-1})
ξ_m	P mineralisation rate (kg-P ha^{-1} day^{-1})
ξ_{ra}	rapid adsorption rate of P from P_{LB} to P_{AI} (kg-P ha^{-1} day^{-1})
ξ_{sa}	slow adsorption rate of P from P_{AI} to P_{SI} (kg-P ha^{-1} day^{-1})
ρ	density of sediment particles (=2650 kg m^{-3})
σ_{ra}	equilibrium coefficient for rapid adsorption (dimensionless)
ς	fraction of a given particle size class in the top soil (dimensionless)
ϕ	median particle size (μm)
ω	unit stream power (cm s^{-1})
ϖ	critical value of unit stream power (cm s^{-1})
Δl	field drain spacing (m)
Δt	time step (day)
Δx	cell size (m)
Π_{fd}	transfer function for dissolved P transported by field drain flow (dimensioless)

Π_{mp}	transfer function for dissolved P transported by macropore flow (dimensionless)
Π_{sa}	transfer function for dissolved P transported by aquifer recharge flow (dimensionless)
Π_{sr}	transfer function for dissolved P transported by surface runoff (dimensionless)
Ω_{sr}	amount of surface runoff when 63% of dissolved P is transported (m)
A	macroporosity factor (dimensionless)
A_h	energy advected to the water body (MJ m^{-2} day^{-1})
b	rain drop impact attenuation coefficient (dimensionless)
C	initial sediment concentration in the rill flow (kg m^{-3})
$C\%$	volume percent of clay (%)
$C_{DP(rz)}$	concentration of dissolved P in the root zone (kg-P m^{-3})
$C_{PP(ch)}$	concentration of particulate P in the channel bed sediment storage (kg-P kg^{-1})
$C_{PP(top)}$	concentration of particulate P in the top 1 cm of the soil (kg-P kg^{-1})
d_{eq}	equivalent depth in Hooghoudt equation (m)
d_{soil}	depth of the soil layer (m)
d_{sw}	depth of overland surface water (mm)
D	vapour pressure deficit (kPa)
DP_{ch}	amount of dissolved P transported to the downstream by channel flows (kg-P ha^{-1})
DP_{fd}	amount of dissolved P transported from the soil to the channel by field drain flows (kg-P ha^{-1})
DP_{mp}	amount of dissolved P transported from the soil to the channel by macropore flows (kg-P ha^{-1})
DP_{sa}	amount of dissolved P transported from the soil to the aquifer by macropore flows (kg-P ha^{-1})

EGU

DP_{sr} amount of dissolved P transported from the top soil to the channel by surface runoff (kg-P ha^{-1})

E_c transpiration rate of a crop (mm day^{-1})

E_p potential evaporation rate (mm day^{-1})

E_{rc} reference crop transpiration rate (mm day^{-1})

E_s evaporation rate from the soil surface (mm day^{-1})

f infiltration rate (mm hr^{-1})

F accumulated infiltration (mm)

FD sediment detachment by rill flow (kg m^{-1} s^{-1})

G heat conduction into the soil (MJ m^{-2} day^{-1})

h elevation of groundwater table (m)

H saturated thickness of the aquifer (m)

H_c canopy height (m)

I_c canopy interception (mm)

IW_{ch} interstitial water in the channel bed which consists of water in the channel bed sediment storage and in the top 1 cm of the firm channel bed (m^3)

k_θ soil water adjustment factor (dimensionless)

k_d rate coefficient for active organic matter decomposition (day^{-1})

k_e extinction coefficient for solar radiation interception through the canopy

k_{eff} effective hydraulic conductivity of the soil (m h^{-1} or m day^{-1})

k_h rate coefficient for humus mineralisation (day^{-1})

k_{ra} rate coefficient for rapid adsorption of P from P_{LB} to P_{Al} (day^{-1})

k_{sa} rate coefficient for slow adsorption of P from P_{Al} to P_{Sl} (day^{-1})

k_{sat} saturated hydraulic conductivity of the soil (m day^{-1})

k_{TB} temperature adjustment factor for biochemical processes (dimensionless)

k_{TS} temperature adjustment factor for sorption (dimensionless)

k_{unsat}	unsaturated hydraulic conductivity of the soil (m day^{-1})
k_ψ	soil water stress factor (dimensionless)
K_{co}	potential crop coefficient (dimensionless)
KE_l	kinetic energy of leaf drainage from the canopy (J m^{-2})
KE_r	kinetic energy of direct rainfall (J m^{-2})
K_{sat}	saturated hydraulic conductivity of the fast-flowing aquifer layer (m day^{-1})
LAI	leaf area index (m^2 m^{-2})
LIT	LAI equivalent of ground litter (m^2 m^{-2})
LL	combined index of leaf area and ground litter (m^2 m^{-2})
m	soil evaporation coefficient (dimensionless)
M	Michaelis-Menten's half-saturation constant of dissolved P concentration for a given plant (kg-P m^{-3})
n	Averjanov's exponent (dimensionless)
p	period of diurnal temperature variation (=86400 s)
P_{AI}	active inorganic P storage (kg-P ha^{-1})
P_{AO}	active organic P in the soil (kg-P ha^{-1})
P_{LB}	labile P storage (kg-P ha^{-1})
$P_{LB(ch)}$	labile P in the channel (kg-P ha^{-1})
$P_{LB(fd)}$	labile P in the interactive zone between water table and field drains (kg-P ha^{-1})
$P_{LB(mp)}$	labile P in the interactive zone below water table (kg-P ha^{-1})
$P_{LB(sa)}$	labile P in the soil below water table (kg-P ha^{-1})
$P_{LB(top)}$	labile P in the top 1 cm of the soil (kg-P ha^{-1})
PP_{ch}	amount of particulate P transported by downstream channel flows (kg-P)
PP_{sr}	amount of particulate P transported from the soil to the channel (kg-P ha^{-1})

P_{SI} stable inorganic P in the soil (kg-P ha^{-1})

P_{SO} stable organic P in the soil (kg-P ha^{-1})

P_{up} P uptake rate by a given plant (kg-P ha^{-1} day^{-1})

q_r flow rate in a rill (m^3 s^{-1})

q_{sa} amount of water flow from the soil to the aquifer, calculated for individual 0.1% soil water content (m^3)

Q_{ch} downstream channel water discharge (m^3)

Q_{fd} preferential flow through field drains (m^3 day^{-1})

Q_{sa} total water flow from the soil to the aquifer (m^3 day^{-1})

Q_{sr} surface runoff expressed in water depth (m)

R daily rainfall (mm)

R_n net radiation exchange for the free water surface (MJ m^{-2} day^{-1})

s energy slope of water (dimensionless)

S storage coefficient of the aquifer (m m^{-1})

$S\%$ volume percent of sand (%)

S_{ch} sediment transported to downstream by channel flows (kg)

SD splash detachment by rain drop impact (kg ha^{-1})

S_f matric potential of suction at the wetting front (mm)

S_{sr} sediment transported to the channel by surface runoff (kg ha^{-1})

t time (day)

t_T travel time of the recharge flow (day)

T daily mean air temperature (˚C)

T' daily mean soil temperature (˚C)

TC sediment transport capacity of the rill flow (kg m^{-3})

$\bar{u}$ mean flow velocity (cm s^{-1})

U_2 wind speed measured at 2 m above the ground surface (m s^{-1})

$U_{\max}$ maximum rate of P uptake by a given plant (kg-P ha^{-1} day^{-1})

EGU

v settling vecolity of sediment particles (m s^{-1})

V_{ss} volume of the soil layer (m^3)

W_r width of rill flows (m)

z soil depth (m)

References

Arnold, J. G., Williams, J. R., Griggs, R. H., and Sammons, N. B.: SWRRBWQ – A Basin Model for Assessing Management Impacts on Water Quality (Draft), USDA ARS, Grassland, Soil, and Water Research Laboratory, Temple, TX, 1991.

Averjanov, S. F.: About permeability of subsurface soils in case of incomplete saturation, English Collection, 7, 19–21, 1950 (as quoted by Palubarinova, P. Ya.: The theory of ground water movement (English translation by DeWiest, I. M. R.), Princeton University Press, Princeton, NJ, 1962).

Barber, S. A.: Soil-plant interactions in the phosphorus nutrition of plants, in: The Role of Phosphorus in Agriculture, edited by: Khasawneh, F. E., Sample, E. C., and Kamprath, E. J., Am. Soc. Agronomy, Crop Sci. Soc. Am., Soil Sci. Soc. Am., Madison, Wisconsin, US, 591–615, 1980.

Bicknell, B. R., Imhoff, J. C., Kittle, J. L., Jr., Donigian, A. S., Jr., and Johanson, R. C.: Hydrological Simulation Program – Fortran: User's manual for version 11, U.S. Environmental Protection Agency, National Exposure Research Laboratory, Athens, GA, EPA/600/R-97/080, 755 pp., 1997.

Bouraoui, F. and Dillaha, T. A.: ANSWERS-2000 – Nonpoint Source Nutrient Transport Model, J. Environ. Eng., 126, 1045–1055, 2000.

Bowes, M. J., House, W. A., and Hodgkinson, R. A.: Phosphorus dynamics along a river continuum, Sci. Total Environ. 313, 199–212, 2003.

Brakensiek, D. L. and Rawls, W. J.: Effects of agricultural and rangeland management systems on infiltration, in: Modeling Agricultural, Forest and Rangeland Hydrology, ASAE, St. Joseph, Mich., 247, 1988.

A distributed continuous simulation model

B. K. Koo et al.

EGU

Brandt, C. J.: The size distribution of throughfall drops under vegetation canopies, Catena 16, 507–524, 1989.

Brandt, C. J.: Simulation of the size distribution and erosivity of raindrops and throughfall drops, Earth Surface Processes and Landforms 15, 687–698, 1990.

5   Campbell, K. L., Kiker, G. A., and Clark, D. J.: Development and testing of a nitrogen and phosphorus process model for Southern African water quality issues, ASAE Annual International Meeting, 30 July–1 August 2001, Sacramento, CA, USA, paper no. 01-2085, 17, 2001.

Chapman, A. S., Foster, I. D. L., Lees, J. A., Hodgkinson, R. A., and Jackson, R. H.: Particulate phosphorus transport by sub-surface drainage from agricultural land in the UK – Environ-

10   mental significance at the catchment and national scale, Sci. Total Environ., 266, 95–102, 2001.

Cronshey, R. G. and Theurer, F. D.: AnnAGNPS - Non-point pollutant loading model, Proceedings of the 1st Federal Interagency Hydrologic Modeling Conference, Las Vegas, Nevada, 19–23 April 1998, 1–9 to 1–16, 1998.

15   Dils, R. M. and Heathwaite, A. L.: The controversial role of tile drainage in phosphorus export from agricultural land, Water Sci. Tech., 39, 55–61, 1999.

Gardner, C. M. K., Cooper, D. M., and Hughes, S.: Phosphorus in soils and field drainage water in the Thame catchment, UK, Sci. Total Environ., 282/283, 253–262, 2002.

Gburek, W. J. and Sharpley, A. N.: Hydrologic controls on phosphorus loss from upland agri-

20   cultural watersheds, J. Env'tal. Qual., 27, 267–277, 1998.

Gilley, J. E., Kottwitz, E. R., and Simanton, J. R.: Hydraulic characteristics of rills, Trans. ASAE, 33, 1900–1906, 1990.

Govers, G.: Empirical relationships on the transport capacity of overland flow, Proceedings of the Jerusalem Workshop, Erosion, Transport and Deposition Processes, March–April 1987,

25   IAHS Publ. No. 189, 45–63, 1990.

Green, W. H. and Ampt, G. A.: Studies on soil physics, 1. The flow of air and water through soils, J. Agric. Sci., 4, 11–24, 1911.

Gupta, A., Destouni, G., and Jensen, M. B.: Modelling tritium and phosphorus transport by preferential flow in structured soil, J. Contam. Hydrol., 35, 389–407, 1999.

30   Haygarth, P. M. and Jarvis, S. C.: Soil derived phosphorus in surface runoff from grazed grassland lysimeters, Water Res., 11, 140–148, 1997.

Heathwaite, A. L. and Dils, R. M.: Characterising phosphorus loss in surface and subsurface hydrological pathways, Sci. Total Env., 251/252, 523–538, 2000.

A distributed continuous simulation model

B. K. Koo et al.

Title Page

Abstract	Introduction
Conclusions	References
Tables	Figures

◀◀   ▶▶

◀   ▶

Back   Close

Full Screen / Esc

Print Version

Interactive Discussion

EGU

Heathwaite, A. L., Haygarth, P. M., and Dils, R.M.: Pathways of phosphorus transport, in: Agricultural Phosphorus in the Chesapeake Bay Watershed – Current Status and Future Trends, edited by: Sharpley, A. N., USDA-ARS Chesapeake Bay Consortium, 2000.

Hooghoudt, S. B.: Bijdrage tot de kennis van enige natuurkundige grootheden van de grond, Verslagen van Landbouwkundiege Onderzoekingen, 46, 515–707, 1940.

House, W. A., Denison, F. A., and Armitage, P. D.: Comparison of the uptake of inorganic phosphorus to a suspended and stream bed-sediment, Water Res., 29, 767–779, 1995.

Jones, C. A., Cole C. V., Sharpley A. N., and Williams, J. R.: A simplified soil and plant phosphorus model, I. Documentation, Soil Sci. Soc. Am. J. 48, 800–805, 1984.

Kang, S, Kim, S., Oh, S., and Lee, D.: Predicting spatial and temporal patterns of soil temperature based on topography, surface cover and air temperature, Forest Ecol. Manage. 136, 173–184, 2000.

Lilly, A., Hudson, G., Birnie, R. V., and Horne, P. L.: The inherent geomorphological risk of soil erosion by overland flow in Scotland, Scottish Natural Heritage Research, Survey and Monitoring Report No. 183, 2002.

Lloyd, J. and Taylor, J. A.: On the temperature dependence of soil respiration, Functional Ecology 8, 315–323, 1994.

Maidment, D. R.: Developing a spatially distributed unit hydrograph by using GIS, HydroGIS 93: Application of GIS in Hydrology and Water Resources, IAHS Publ. No. 211, 181–192, 1993.

McGechan, M. B.: Effects of timing of slurry spreading on leaching of soluble and particulate inorganic phosphorus explored using the MACRO model, Biosyst. Eng., 83, 237–252, 2002.

McGechan, M. B., Jarvis, N. J., Hooda, P. S., and Vinten, A. J. A.: Parameterization of the MACRO model to represent leaching of colloidally attached inorganic phosphorus following slurry spreading, Soil Use Manage, 18, 61–67, 2002.

Mein, R. G. and Larson, C. L.: Modeling infiltration during a steady rain, Water Resour. Res., 9, 384–394, 1973.

Menzel, R. G.: Enrichment ratios for water quality modeling, in: CREAMS – A field scale model for chemicals, runoff, and erosion from agricultural management systems, edited by: Knisel, W. G., USDA Conserv. Res. Rept. No. 26, 486–492, 1980.

Morgan, R. P. C., Quinton, J. N., Smith, R. E., Govers, G., Poesen, J. W. A., Auerswald, K., Chisci, G., Torri, D., Styczen, M. E., and Folly, A. J. V.: The European Soil Erosion Model (EUROSEM) – Documentation and user guide, Cranfield University, UK, 1998.

Needelman, B. A., Gburek, W. J., Sharpley, A. N., and Petersen, G. W.: Environmental management of soil phosphorus: Modeling spatial variability in small fields, Soil Sci. Soc. Am. J. 65, 1516–1522, 2001.

Neitsch, S. L., Arnold, J. G., Kiniry, J. R., and Williams, J. R.: Soil and water assessment tool – Theoretical documentation, Grassland, Soil and Water Research Laboratory, Agricultural Research Service, http://www.brc.tamus.edu/swat, 2001.

Rauws, G. and Govers, G.: Hydraulic and soil mechanical aspects of rill generation on agricultural soils, J. of Soil Sci., 39, 111–124, 1988.

Rawls, W. J., Brakensiek, D. L., and Savabi, R.: Infiltration parameters for rangeland soils, J. Range Manage, 42, 139–142, 1989.

Shuttleworth, W. J.: Evaporation, in: Handbook of Hydrology, edited by: Maidment, D., McGraw-Hill, 4.1–4.53, 1993.

Simard, R. R., Beauchemin, S., and Haygarth, P. M.: Potential for preferential pathways of phosphorus transport, J. Environ. Qual., 29, 97–105, 2000.

Smith, R, Goodrich, D., and Quinton, J.: Dynamic, distributed simulation of watershed erosion: The KINEROS2 and EUROSEM models, J. Soil Water Conserv., 50, 517–520, 1995.

Theurer, F. D. and Cronshey, R. G.: AnnAGNPS – Reach routing processes, Proceedings of the First Federal Interagency Hydrologic Modeling Conference, Las Vegas, Nevada, 19–23 April 1998, 1-25–1-32, 1998.

Viney, N. R., Sivapalan, M., and Deeley, D.: A conceptual model of nutrient mobilisation and transport applicable at large catchment scales, J. Hydrol., 240, 23–44, 2000.

Wade, A. J., Whitehead, P. G., and Butterfield, D.: The integrated catchments model of phosphorus dynamics (INCA-P), a new approach for multiple source assessment in heterogeneous river systems: model structure and equations, Hydrol. Earth Sys. Sci., 6, 583–606, 2002, SRef-ID: 1607-7938/hess/2002-6-583.

Walling, D. E., Webb, B. W., and Russell, M. A.: Sediment-associated nutrient transport in UK rivers. in: Freshwater contamination, Proc. Rabat Symp., April–May 1997, Int. Assoc. Hydrol. Sci.; IAHS Publ. No. 243, 69–81, 1997.

Williams, J. R.: Sediment-yield prediction with universal equation using runoff energy factor, in: Present and Prospective Technology for Predicting Sediment Yield and Sources, ARS, S-40 US Gov. Print Office, Washington, D.C., 244–252, 1975.

A distributed continuous simulation model

B. K. Koo et al.

|	
Title Page	
Abstract	Introduction
Conclusions	References
Tables	Figures
◄◄	►►
◄	►
Back	Close
Full Screen / Esc	

Print Version

Interactive Discussion

EGU
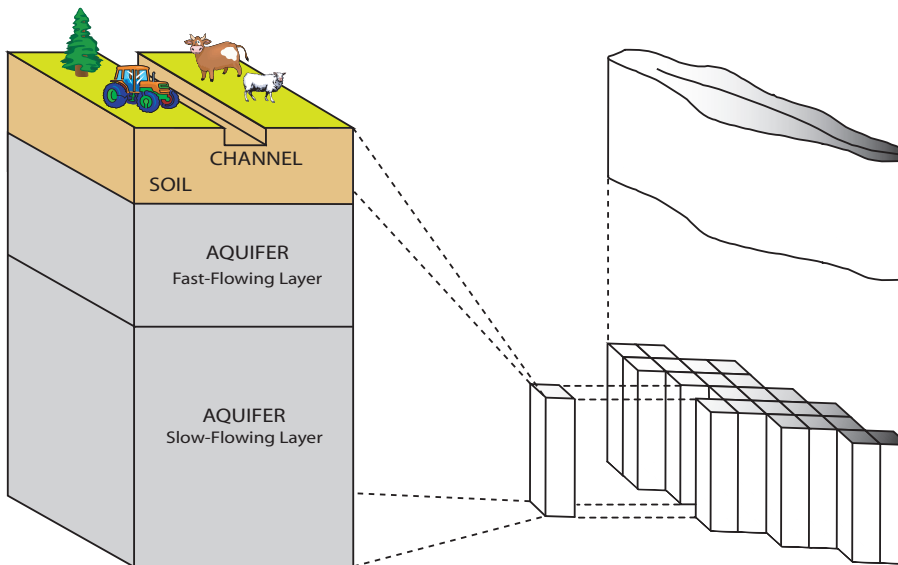
Fig. 1. Representation of a catchment in CAMEL. A catchment is represented using a network of square grid cells each of which represents the corresponding soil-aquifer column within the catchment. Based on this structure, the model simulates both surface and subsurface processes explicitly.

EGU
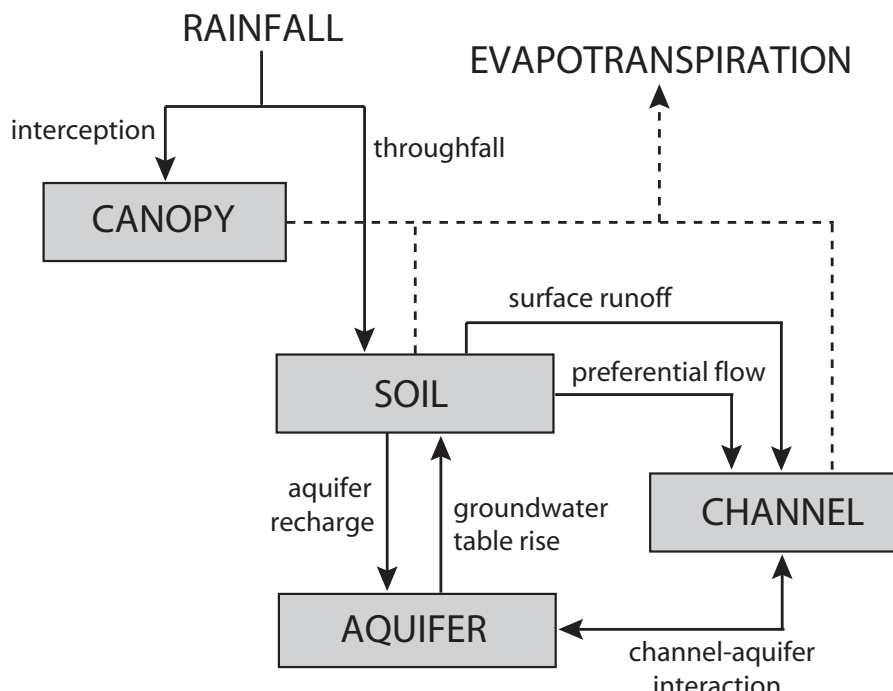
Fig. 2. Water storages and hydrological processes within a cell.

EGU

EGU
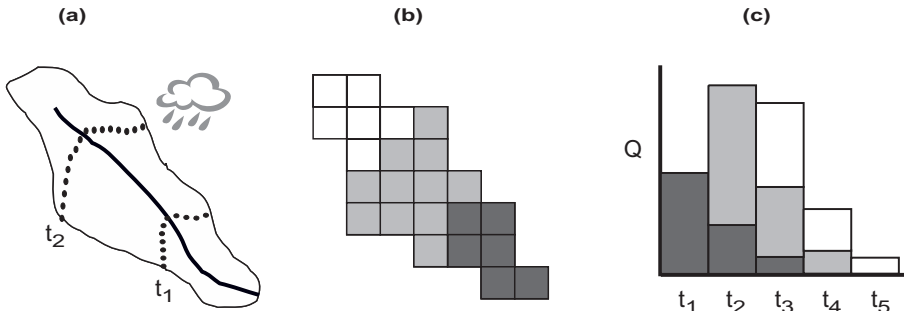
Fig. 3. Channel routing by a spatially distributed unit hydrograph approach: **(a)** a catchment can be divided into areas of isochrones; **(b)** isochrones are determined according to the mean travel time of channel water flows from a given cell to the catchment outlet; **(c)** unit hydrograph ordinates from individual isochrone areas are linearly superposed to estimate the total discharge.
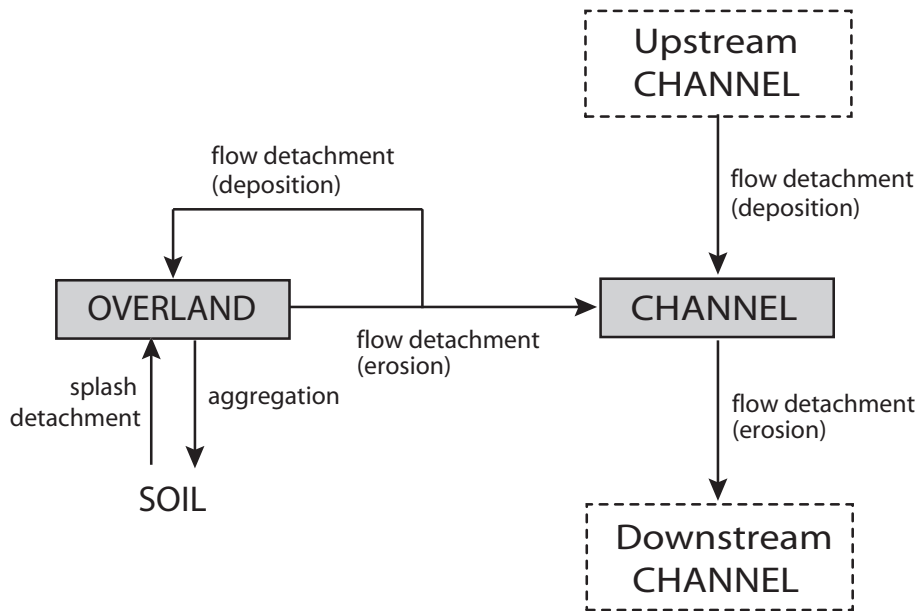
Fig. 4. Sediment storages and sediment transport processes within a cell. Sediment storages are defined for each of the four particle size classes, i.e. clay, silt, fine sand and coarse sand.
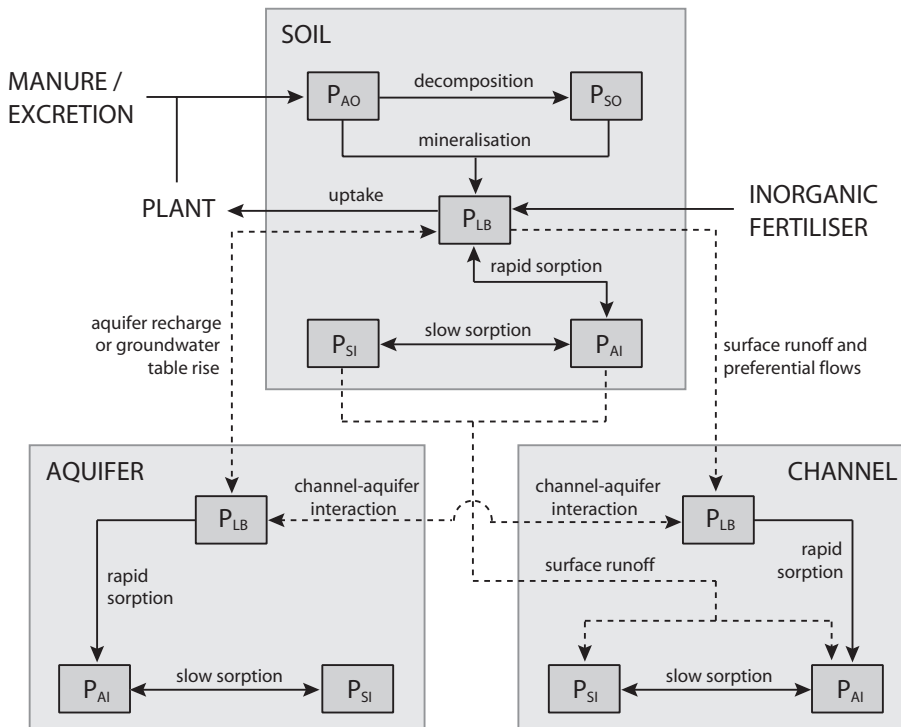
Fig. 5. Intra-cell P transformation and transport processes between P storages (P_{AO}=active organic P; P_{SO}=stable organic P; P_{LB}=labile P; P_{AI}=active inorganic P; P_{SI}=stable inorganic P).

EGU
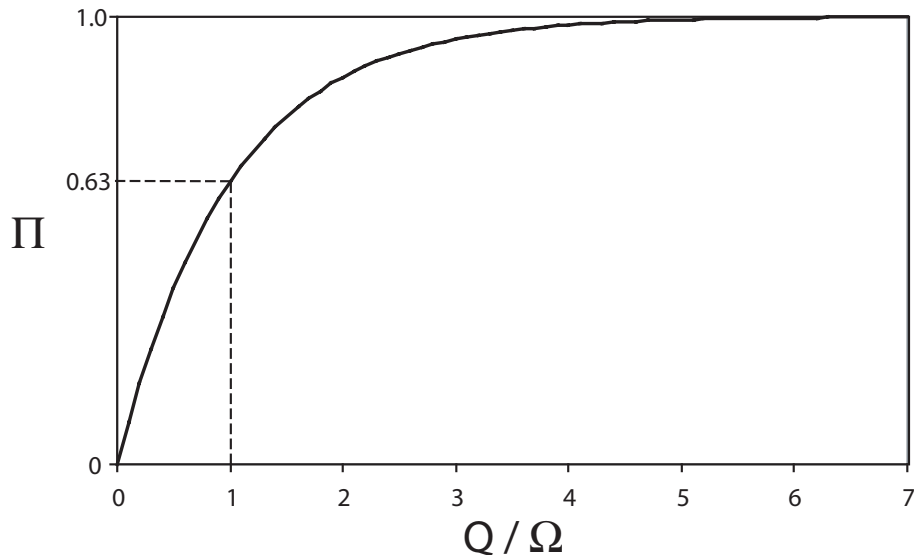
Fig. 6. A transfer function used in the model for estimating transport of dissolved P. When $Q=\Omega$, it is assumed that 63% of dissolved P in the "interactive zones" around the preferential pathways is transported.